CIMAC CONGRESS 25
ZURICH, MAY 19 – 23, 2025

2025 | 234

High-reactivity fuel spray ignition pre-chamber: achieving rapid combustion in ammonia marine engine

Fuels - Alternative & New Fuels

Zhuohang Li, Shanghai Jiao Tong University

Jinze Li, Shanghai Jiao Tong University
Yezeng Fan, Shanghai Jiao Tong University
Tiankui Zhu, Shanghai Jiao Tong University
Zhan Gao, Shanghai Jiao Tong University
Lei Zhu, Shanghai Jiao Tong University
Zhen Huang, Shanghai Jiao Tong University

ABSTRACT

Ammonia (NH3), as a carbon-free fuel, has attracted attention for its great potential to reduce carbon emissions in the shipping industry. However, its poor combustion characteristics make it challenging to apply in marine engines. In this study, both experimental and numerical simulations were conducted to explore enhanced ammonia combustion using the high-reactivity fuel spray ignition pre-chamber. Flame dynamics in the pre-chamber under different conditions were observed using a constant volume combustion chamber system with a visible pre-chamber. The effects of different fuel injection quantity and ammonia-air mixture equivalence ratios on the ignition process in the pre-chamber and main-chamber were analyzed. Large eddy simulations were performed under temperature and pressure relevant to typical marine engines. The combustion process and the variation of jet properties in the spray ignition pre-chamber were investigated. Jet ignition mechanism differences between this type pre-chamber and hydrogen-assisted spark ignition pre-chamber were found. The results indicate that the high-reactivity fuel spray ignition pre-chamber offers advantages in rapid ignition, enhanced combustion, and greater combustion stability. Preliminary numerical simulation results for a high-speed marine engine show that this mode is expected to achieve high thermal efficiency and low unburned ammonia emissions at ultra-high ammonia substitution rates.

1 INTRODUCTION

Ammonia has gained significant attention as a carbon-free fuel for marine engines [1]. However, its utilization presents challenges due to low flame speed, high ignition energy, and high auto-ignition temperature [2]. These characteristics result in lower engine efficiency and higher emissions of unburned ammonia. Two combustion mode have been proposed for enhancing ignition and accelerating in-cylinder combustion process [3]. One is liquid ammonia and pilot fuel high pressure injection under extreme conditions [4]. The other one is using pilot fuel jet [5] or burned gas jet [6] to ignite the ammonia-air mixture under milder conditions. For the latter, experimental studies have shown pilot fuel ignition struggles to simultaneously support high ammonia substitution rate and high thermal efficiency, with limited potential to reduce greenhouse gas emission [7],[8]. Pre-chamber jet ignition, by contrast, is considering as a promising technology. This technology works by creating localized thermodynamic and thermochemical stratification in the combustion chamber, which trigger thermal runaway rapidly and form stable flame core. It also boosts turbulence, speeding up flame propagation [9].

Recent studies have focused extensively on applying pre-chamber to ammonia engines, with some researchers aiming to achieve pure ammonia combustion. Meng et al. [10] and Liu et al. [11] conducted both experimental and numerical studies on pure ammonia jet ignition using constant volume combustion chamber and small-bore engine. The results showed that this mode struggled to achieve stable and rapid ignition. The engine's efficiency was low, and unburned ammonia emissions were unacceptably high. Zhou et al. [12] proposed the use of other fuels (such as hydrogen, natural gas and gasoline) to improve reactivity in the pre-chamber, naming this as the Reactivity controlled turbulent jet ignition mode. Among potential fuels, hydrogen is often preferred due to its high reactivity and carbon-free characteristic [13]. For example, Wang et al. [14] developed an Ammonia combustion using hydrogen jet ignition engine, achieving an indicated thermal efficiency of 42.5% with 97% ammonia substitution rate. However, their subsequent research [15] highlighted challenges with this mode.

Currently, most researchers rely on high-octane fuels to improve pre-chamber reactivity, using spark ignition to initiate premixed flame propagation. When the fuel properties shift to be diesel-like, low-temperature reactivity and self-ignition characteristics are expected to significantly alter the flame dynamics in the pre-chamber. These changes will have substantial impacts on the jet ignition process and engine performance. It is important to note that none of the effects discussed above have been fully explored. Furthermore, research on jet ignition mechanisms at temperatures and pressures relevant to marine engines is very limited. This paper aims to address this gap. Research

In this study, the ignition mechanism of high-reactivity fuel spray ignition pre-chamber will be discussed. The mechanisms of this type and spark ignition pre-chamber will also be compared under the relevant conditions of marine engines. Additionally, we will explore the potential application of this approach in ammonia marine engines, aiming to achieve ultra-high ammonia substitution rate.

2 RESEARCH METHOD

2.1 Experiment Setup

To better understand the fundamental characteristics of high-reactivity fuel spray ignition pre-chamber, a Constant Volume Combustion Chamber (CVCC) system with visible pre-chamber was developed. Figure 1 depicts the system's appearance and chamber dimensions, featuring an internal diameter of 230 mm and an effective volume of approximately 4.45 L. Considering the direction of spray and fuel volume matching, the effective volume of the visualized pre-chamber is designed to be 184 mL, accounting for approximately 3.97% of the total volume. The observation window is made of sapphire glass with a thickness of 8 mm, ensuring both durability and optical clarity. The pre-chamber is connected to the main-chamber via a passage that is 17 mm long and 8 mm in diameter.

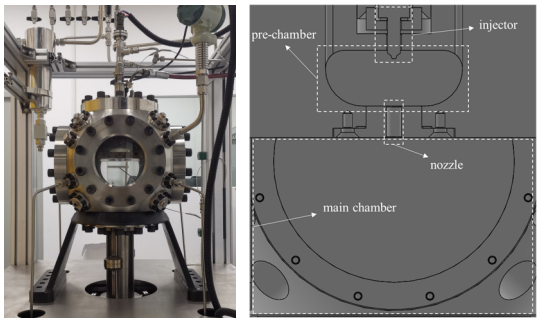

Figure 1. Constant Volume Combustion Chamber system with Visible pre-chamber

Airflow, regulated by a flowmeter, is directed through a heating module that raises the internal temperature to create high-temperature initial atmosphere of about 750 K. This setup ensures the chamber provides a stable high-temperature environment for the experiments. The data

acquisition system includes Kistler 6024A pressure sensor, 2082B12 charge signal conditioning platform, 5064E11 charge signal amplifier, and Pico5442D high-resolution oscilloscope. This configuration allows real-time, accurate measurement of pressure changes within the CVCC. Optical data is captured using a Phantom V2012 high-speed camera, which supports a maximum resolution of 1280×800 at 22,600 frames per second (fps). For the experiment, the optical test parameters were set to 768×768 resolution at 30,000 fps. For precise measurements, the pre-chamber is equipped with a Kistler 6024A pressure sensor and thermocouples to monitor internal pressure and temperature accurately.

The operating process of the system is as follows: First, the high-temperature environment in both chambers is established using the intake heating system. Ammonia is then introduced at low pressure, followed by high-pressure air. Once the temperatures in the main-chamber and the pre-chamber are equalized, pressure measurement, high-speed photography, and diesel fuel injection are initiated simultaneously using a synchronized triggering device. Diesel fuel is injected into the pre-chamber via a high-pressure common rail system, where it increases the pressure and ignites the ammonia-air mixture under high-temperature and high-pressure conditions. The tests in this study were conducted at 1 MPa and 673K.

2.2 Numerical Simulation Method

The numerical simulation study presented in this paper aims to investigate the jet ignition mechanism of high-reactivity fuel spray ignition pre-chamber, specifically under thermodynamic conditions near the TDC of typical marine engines. These conditions are difficult to replicate in current experimental setups. Following the clarification of the ignition mechanism, the study explores the combustion and emission performance of an ammonia high-speed marine engine equipped high-reactivity fuel spray ignition pre-chamber. All simulations were conducted using the CONVERGE (v4.0) code package, which has demonstrated exceptional capability in predicting flow and combustion under engine-related conditions worldwide.

In studying the jet ignition mechanism, large eddy simulation (LES) was employed to accurately replicate the turbulence field structure and turbulent kinetic energy levels, closely matching real conditions. LES has been shown to be crucial in examining high-pressure spray ignition mechanisms, as demonstrated in the work of Pei et al [16]. The geometric model and mesh used in the simulations are shown in Figure 2, where the pre-chamber is 4.5 mL, the main-chamber is 135 mL, and the nozzle is round with diameter of 2mm/3mm. To model the spray ignition process in the pre-chamber, we closely followed the framework developed by Kaario et al. [17], replicating their LES research as much as possible to ensure the combustion process inside the chamber was accurately represented. For further numerical details, the reader is referred to their original work. Additionally, the LES framework developed by Poinsot et al. [18] was used to model the jet ignition process.

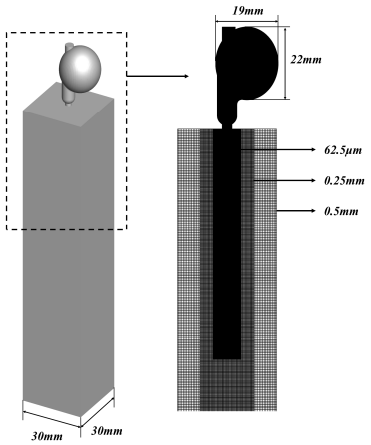

Figure 2. Geometry and mesh of computational domain with dimensions

Two key points should be emphasized: First, to address the flow state in both the near-field and far-field regions of the high-temperature gas jet, fix embedded and adaptive mesh refinement strategy were implemented. In the core region of the jet, the grid size was set as 62.5 μm, resulting in about 20 million grids for this case. Second, as the fluid passes through the nozzle, it is accelerated and subjected to shear, resulting in strong turbulence. Based on the DNS results of Poinsot et al. [19], most of the region affected by the jet exhibits broken reaction flame, making it challenging for flamelet model to capture its key characteristics. In contrast, the ideal jet-stirred reactor model provides a more accurate representation. Therefore, in this study, the SAGE solver from the CONVERGE code package was used to ensure the highest possible accuracy.

Since different fuels (hydrogen and n-heptane) were involved, two distinct kinetic mechanisms were employed for the simulations. The first mechanism is the NH_3/n-heptane mechanism, which consists of 57 species and 159 reactions, recently developed by Nilsson et al. [20]. This mechanism is based on the detailed results from Glarborg and Ju et al. [21] and has shown high prediction accuracy for both ignition delay time (IDT) and species concentrations. The second

mechanism is the NH_3/H_2 mechanism, which includes 31 species and 203 reactions and was developed by Stagni et al. [22]. This mechanism currently provides the best predictions for flame speed and species concentrations.

For the simulations, the thermodynamic condition in the computational domain was set to 8 MPa, 1000 K, and the ammonia-air mixture equivalence ratio to 0.8. In the high-reactivity fuel spray ignition pre-chamber, the n-heptane injection mass was 3.6 mg, with an injection pressure of 50 MPa. The mass of hydrogen in the H2-assisted spark ignition pre-chamber was 1.35 mg (molar fraction in the pre-chamber is 0.142). It is similar with the hydrogen molar fraction calculated in the research work of Wang et al. [15] for a real engine.

The high-reactivity fuel spray ignition pre-chamber developed by our research group is currently in the installation and testing phase. To demonstrate its potential performance, we use numerical simulations. In this paper, we will focus on a single-cylinder, four-stroke marine high-speed engine. Due to the high computational cost of using the LES for engine performance analysis, we have opted for the RANS instead. The modeling process and mechanism selection follow the approach outlined by Zhou et al. [23] The specific engine parameters and computational models are provided in Tables 1 and 2.

Table 1. Parameters of the engine

Parameters	Value
Engine	Single-cylinder, four-stroke, four-valve
Air intake method	Turbocharging, intercooler
Total displacement (L)	2.13L
Bore (mm)	130
Stroke (mm)	161
Conn. Rod length (mm)	245
Compression ratio	17
Engine Speed (rpm)	1500
Intake valve opening (IVO) (°CA ATDC)	338
Intake valve closing (IVC) (°CA ATDC)	−139
Exhaust valve opening (EVO) (°CA ATDC)	111
Exhaust valve closing (EVC) (°CA ATDC)	−329

Table 2. Sub-models used for spray and combustion modeling

Phenomenon	Model	Refs.
Spray breakup	Kelvin Helmholtz (KH) and Rayleigh Taylor (RT) model	[24]
Droplet collisions	NTC model	[25]
Droplet evaporation	Frossling model	[26]
Turbulence dispersion and droplet coalescence	O'Rourke's model	[27]
Turbulence	RNG k-ε model	[28]
Combustion	SAGE detailed chemistry solver Chemical Kinetics model	[29]

For the simulations in this paper, three typical load conditions were selected. The intake temperature was set to 303 K, and the intake pressures were 1.35 bar, 1.83 bar, and 2.1 bar. The control total equivalence ratio was fixed at 0.8, with a pre-chamber injection of 6 mg. The ammonia substitution rates for the three load conditions were 95.0%, 96.5%, and 97.0%, respectively.

3 EXPERIMENT RESULT AND DISCUSSION

3.1 The Influence of Fuel Injection Quantity on Ignition process

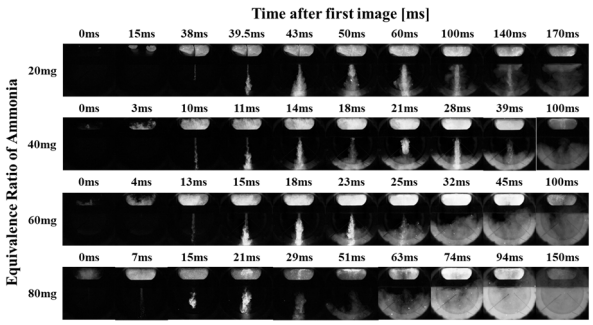

Figure 3: The influence of fuel injection quantity on diesel ignition in pre-chamber and jet ignition process in main chamber

High-speed photography was used to investigate the diesel ignition and the ammonia combustion process. As shown in Figure 3, when the diesel injection quantity in the pre-chamber is relatively low (20 mg), approximately 38ms after injection, the flame front reaches the nozzle. During this phase, the burnt gas is cooled and accelerated as it passes through the nozzle and enters the main-chamber, causing the brightness of the jet flame to significantly decrease. During the throttling process, the flame temperature and pressure are relatively low, which prevents the flame from filling the entire nozzle section. The jet flame's diameter is much smaller than the nozzle diameter, and the flame tip continually extinguishes, being

replenished by the subsequent jet. At 39.5ms, ignition of ammonia begins at the head of the jet. As the jet flame develops downward, it also starts to propagate radially. By 50ms, the first jet flame is interrupted and can no longer sustain a flame at the bottom of the chamber. Simultaneously, a second jet flame is generated in the pre-chamber and shoots downward through the nozzle. Compared to the first jet, the second jet flame maintains a relatively high intensity after passing through the nozzle's cooling effect, due to continued combustion in the pre-chamber. This second jet carries large amount radicals and high-temperature species into the main-chamber. The high-temperature and high-pressure environment created by the heat release in the pre-chamber allows the second jet to fill the entire nozzle. The second jet lasts for about 90ms (from 50ms to 140ms). During this time, new flame cores continuously form in the pre-chamber and are transported to the nozzle. As the flames exit the nozzle and reach the bottom of the main-chamber, the wide-range ammonia/air mixture is ignited, and the flame propagates radially. After about 140ms, the jet disappears, but the ammonia flame in the main-chamber continues to propagate radially along the entire jet axis.

As shown in the second row of images in Figure 3, increasing the prechamber fuel injection quantity to 40 mg causes flame dynamic transition. With more high-reactivity fuel and longer injection duration, the initial flame cores become more widely distributed. The initial jet flame, though similar to the 20 mg case, has a larger flame radius. The first jet flame effectively ignites the ammonia/air mixture at the bottom of the main-chamber. Once ignition in the main-chamber occurs, the flame propagates upward from the bottom. At 18ms, the first jet becomes unsustainable, and the second jet is emitted from the nozzle. The high-speed jet flame has a shorter retention time in the middle of the main chamber, making it less effective for sustained ignition. However, the energy accumulated in the pre-chamber continues to promote combustion at the bottom of the chamber through the jet. As a result, flame propagation in the main-chamber continues to develop upwards from the bottom. When the fuel injection quantity in the prechamber is further increased to 60mg, the jet flame transfers all the effective energy to the main chamber through a single jet within 12ms (from 13ms to 25ms). No second jet is observed in this case. As the jet flame becomes faster, it becomes more difficult to ignite the ammonia/air mixture in the main-chamber.

When the fuel injection quantity in the pre-chamber was further increased to 80 mg, the initial flame core in the pre-chamber became more extensive. However, the equivalence ratio is too high, leading to significant quenching as the flame passed through the nozzle due to heat loss and high strain rate. This made it difficult to form a stable jet flame, and instead, the flame entered the main-chamber as a high-temperature jet. At this stage, weak combustion in the pre-chamber lead to weak jet penetration capability. High-temperature Incomplete reaction products began to accumulate and ignited in the middle of the main-chamber. However, the flame generated in the center could not directly ignite the surrounding ammonia, which remained relatively inert. Instead, the flame propagated downward along the hot jet, tracing back to the pre-chamber. This flame in the main - chamber acted as an ignition source. As it reached the bottom of the chamber, it ignited the mixture of ammonia and early jet substances, causing the flame to propagate upward from the bottom. It is noteworthy that despite the pre-chamber fuel injection quantity reaching 80 mg, the energy contribution of the diesel was only about 5%. That's mean the lowest ammonia substitution rate is 95%.

3.2 The Influence of Equivalence Ratio on Ignition process

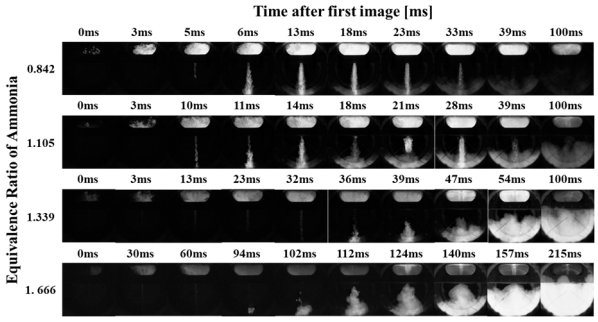

Figure 4: The influence of ammonia-air mixture equivalence ratio on diesel ignition in pre-chamber and jet ignition process in main chamber

As shown in Figure 4, when the equivalence ratio of ammonia-air mixture is 0.842 or 1.105, there is sufficient oxygen, and diesel combustion in the prechamber occurs relatively quickly after injection. The jet flame shape is well-maintained, with a high jet velocity and short duration. The ammonia flame in the main-chamber primarily relies on accumulation at the bottom to form a flame core, propagating upward from the bottom. When the equivalence ratio increases to 1.339, the diesel auto-ignition became more difficult. The jet flame weakens, and after ignition in the middle and lower parts of the jet, it fails to propagate. The flame in the chamber still propagates upward from the bottom. When equivalence ratio reaches 1.666, the combustion process in the pre-chamber weakens further, and the jet flame becomes very weak. The jet gradually decelerates, struggling to penetrate

the entire main chamber. As a result, ignition event occurs in the middle of the chamber (from 94ms to 102ms). Notably, compared to the case with an equivalence ratio of 1.339 (third row of Figure 4) and fuel injection quantity of 80 mg (fourth row of Figure 3), the middle ignition at an equivalence ratio of 1.666 (fourth row of Figure 4) directly ignites the surrounding mixture, enabling flame propagation while the bottom flame continues to propagate upward. In contrast, the middle ignition in the other two cases cannot sustain further development, which may indicate the reduced ignitability of high equivalence ratio mixtures.

4 LARGE EDDY SIMULATION RESULTS AND JET IGNITION MECHANISMS AT ENGINE-RELEVANT CONDITIONS

The aforementioned experiments provide a general understanding of the basic characteristics of the high-reactivity fuel spray ignition pre-chamber. However, achieving thermodynamic conditions near the TDC of typical marine engines remains challenging in current experiments. Additionally, the high transient nature of the jet ignition process makes it difficult to use advanced optical techniques, such as PLIF, which could provide deeper insights into the combustion dynamics. Therefore, large eddy simulation under engine-relevant conditions is crucial for a more thorough understanding of the jet ignition process.

4.1 Combustion processes in pre-chamber and jet properties

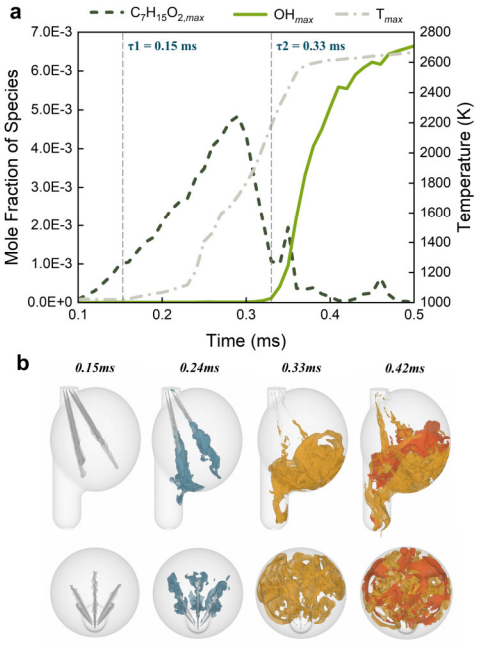

Figure 5: a. The maximum variation in key intermediate products (RO_2 and OH) and temperature during the ignition process in the pre-chamber. b. Iso-surfaces for each important component in the pre-chamber. (gray: X_{NC7H16}=0.1, blue: $X_{C7H15O2}$=0.001, yellow: X_{CO}=0.1, orange: X_{OH}=0.001)

The thermodynamic, thermochemical, and hydrodynamic properties of the jet play a crucial role in determining its ignition mechanism and effectiveness. Therefore, understanding the combustion process in the spray ignition pre-chamber system is particularly important. As illustrated in the figure 5, the entire process can be divided into three stages.

In the first stage, the liquid fuel is injected and rapidly atomized and evaporated. The edge of the fuel jet experiences shear and instability, leading to rapid mixing with the surrounding gas, forming a locally rich mixture in the pre-chamber. In this mixing zone, the low-temperature reactions occur, and the concentration of RO_2 radicals increases. However, due to the limited heat release, the temperature remains nearly constant. In the second stage, the accumulation of RO_2 radicals triggers the appearance of cool-flame in the reaction zone, which causes the temperature to rise rapidly, transitioning the flame into a warm-flame. The continuing rise in temperature leads to partial oxidation and pyrolysis of long carbon-chain species in the high equivalence ratio region near the wall. This results in an increase in the concentration of substances such as CO, H_2, and CH_4. Once the temperature and free radical concentrations reach a critical level, the third stage begins. This triggers high-temperature ignition in the pre-chamber, creating flame front that continuously ignites the ammonia-air mixture above.

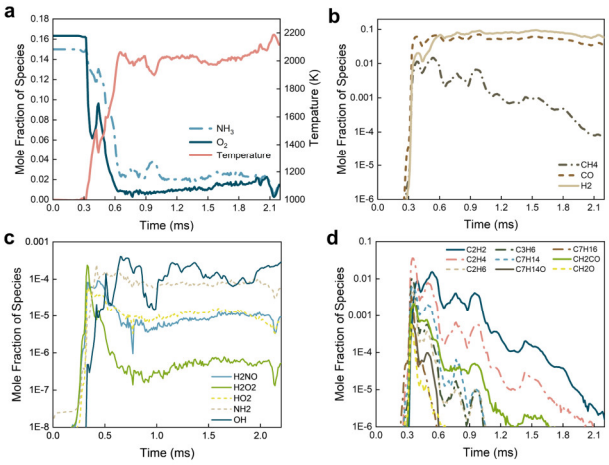

Figure 6 Variation of thermochemical properties in the pre-chamber jet

The combustion characteristics in the pre-chamber make the thermochemical properties of the jet

stage-specific. Figure 6 shows the average values of temperature and the concentration of species at the jet hole exit. It can be observed that in the first stage, the evaporation of fuel causes a slight decrease in temperature in the pre-chamber, and a reverse jet forms along the jet hole. As the low-temperature reactions start, the pressure in the pre-chamber begins to rise, causing the jet to shift and become rich in pyrolysis and low-temperature products. Shortly after the combustion in the pre-chamber enters the second stage, the jet contains some macromolecules (e.g., C_7H_{16} and C_7H_{14}), but their concentration rapidly decreases, and smaller molecules such as hydrocarbons (e.g., CH_4, C_2H_2, and C_2H_4), hydrogen, and carbon monoxide become the main components. Between 0.3ms to 0.6ms, the combustion enters the high-temperature phase, which leads to a gradual increase in jet temperature and a decrease in ammonia and oxygen concentrations. During this phase, the HO_2, $H2O_2$, and H_2NO radicals, which indicate the interaction of high-temperature ignition and low-temperature reactions of carbon-based fuels, also decrease. After 0.6ms, CO and H_2 from the high-equivalence ratio combustion of n-heptane remain in large quantities in the pre-chamber and are discharged with the jet, while the concentration of hydrocarbon fractions gradually decreases. The jet temperature and the concentration of other components stabilize, marking the transition of combustion in the pre-chamber to being dominated by ammonia combustion.

4.2 Jet ignition process and mechanism

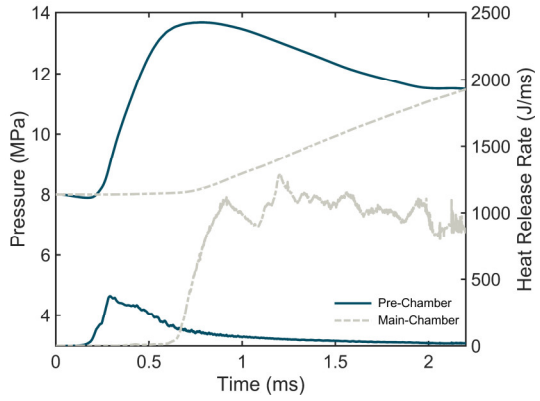

Figure 7. Pressure and heat release rate in the main-chamber and pre-chamber during the jet ignition process (high-reactivity fuel spray ignition pre-chamber)

The formation of the jet is primarily driven by the pressure difference between the inside and outside of the pre-chamber. When high-temperature ignition occurs within the pre-chamber, the pressure inside increases rapidly, pushing the gas toward the main-chamber. However, the narrow nozzle orifice restricts the maximum flow rate, allowing the pressure difference to build up over time, resulting in a continuous jet of high-temperature gas. As shown in Figure 8 & Figure 9, the nozzle diameter is 2 mm, with a jet velocity and Reynolds number at the outlet reaching 800 m/s and 200,000, respectively. When the jet contacts the ammonia-air mixture in the main-chamber, the strong shear forces generate high-speed vortices at the jet's edge, drawing in the surrounding ammonia-air mixture. As these vortices develop from the near-field to the far-field, they gradually move toward the center of the jet due to instability. As mentioned earlier, the high-temperature jet contains H_2, CO, NH_3, and small hydrocarbons, but the oxygen concentration is low. The jet entrainment pulls in the fresh mixture, restarting the combustion process. Thermal runaway occurs when the local chemical reactions produce heat faster than the flow can lose it, creating a steadily developing flame core. Following this, the pressure in the pre-chamber decreases as the heat release rate drops, leading to a reduction in both the mixing and entrainment abilities of the jet. This causes the heat release rate in the main-chamber to decrease as well. When the pressure in the main-chamber exceeds that in the pre-chamber, the jet reverses, entering an oscillatory phase.

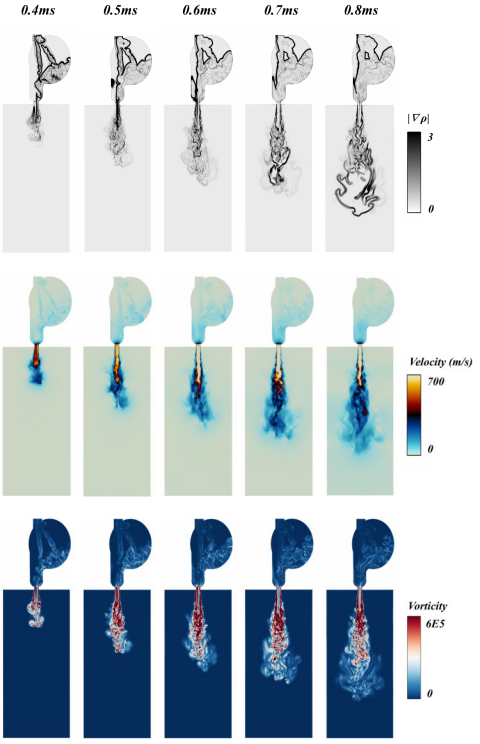

Figure 8. Hydrodynamic characteristics of the jet ignition process with 2 mm diameter nozzle

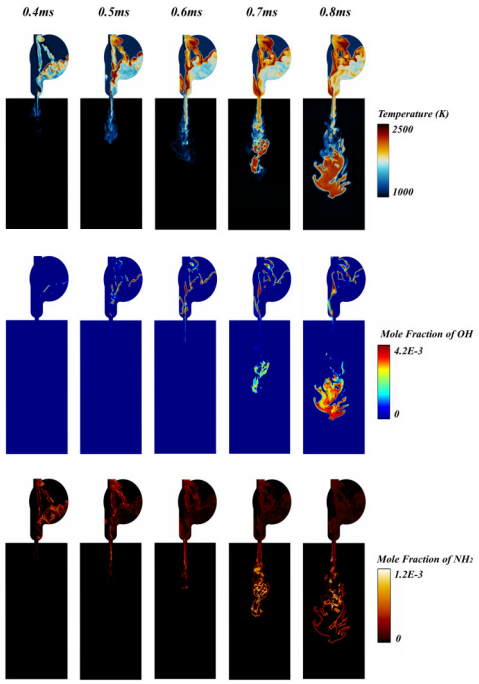

Figure 9. Thermochemical characteristics of the jet ignition process with 2 mm diameter nozzle

When the diameter of the jet hole is increased to 3 mm, as shown in the figure10, the jet ignition process changes noticeably. The jet velocity decreases significantly, and the turbulence produced by the shear force is limited to a smaller area. From a broader perspective, the formation of the flame core occurs 0.2-0.3ms earlier compared to the 2 mm nozzle case, and its position is closer to the nozzle. Comparing these two results provides a deeper understanding of the jet ignition mechanism in the pre-chamber discussed in this study. As the jet entrainment capability decreases and the oxygen concentration in the core region diminishes, the flame core forms much earlier than with the 2 mm nozzle case. This phenomenon can be explained by a reduction in the Karlovitz number (the ratio of the chemical time scale to the Kolmogorov time scale). When the jet orifice is enlarged, the Reynolds number at the jet exit decreases, the vortex size from shear increases, and the Kolmogorov scale vortex dissipation time lengthens. This change is especially significant in the region extending from the jet orifice, causing the region to gradually transition from a fragmented reaction zone flame to a thinner reaction zone on the Williams diagram. This significantly reduces the side effect of turbulent dissipation on flame core formation. Additionally, once the flame core has formed, the pressure difference between the pre-chamber and the main-chamber still exists, so the jet remains uninterrupted. As a result, an interesting phenomenon occurs: the jet continues to pull in the surrounding ammonia-air mixture and undergoes rapid chemical reactions at the location where the flame core was initially formed. The combusted gas retains downward momentum, which "blows bubbles" and pushes the flame front forward, further accelerating the combustion process.

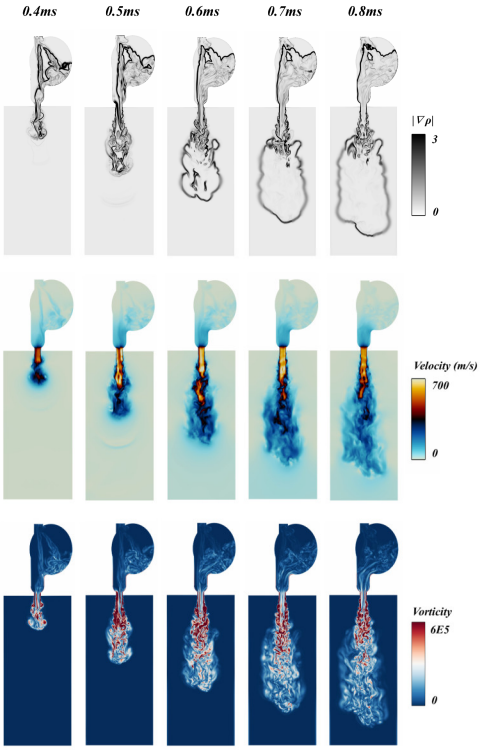

Figure 10. Hydrodynamic characteristics of the jet ignition process with 3 mm diameter nozzle

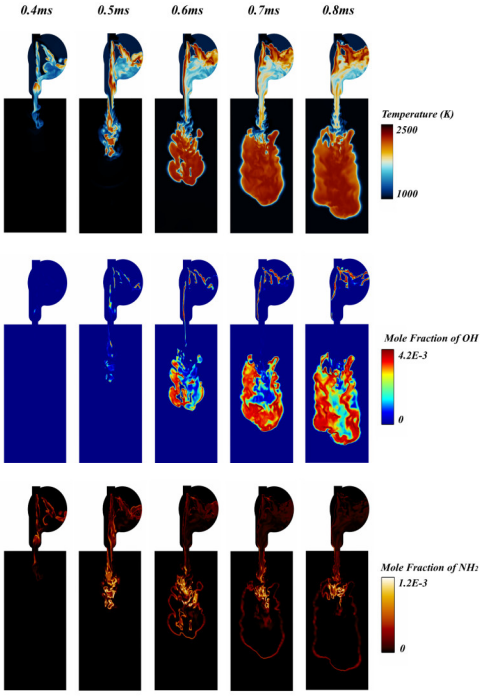

Figure 11. Thermochemical characteristics of the jet ignition process with 3 mm diameter nozzle

4.3 Distinctions of the jet ignition mechanism between high-reactivity fuel spray ignition pre-chamber and hydrogen-assisted spark ignition pre-chamber

In the final subsection of the mechanism discussion, we will examine the differences in macroscopic thermodynamic characteristics and ignition mechanisms between two types of pre-chambers. The nozzle diameter analyzed in this subsection is 3 mm. When spark ignition is used in the pre-chamber, the combustion process can be roughly modeled as spherical flame propagation, with a gradual increase in both the heat release rate and pressure. The ammonia-hydrogen-air mixture in front of the flame front is pushed out of the pre-chamber by the pressure difference, forming a cold jet. Due to the small pressure difference and limited jet entrainment capabilities, the cold jet does not mix extensively with the gas in the main-chamber, instead creating a localized high-activity region downstream of the nozzle. This process lasts about 2ms. As the flame propagates through the nozzle, it directly enters the high-reactivity region, where rapid flame propagation begins. While the initial turbulence along the jet axis is relatively low, the rapidly expanding flame creates stronger vortex motion, which accelerates energy and material diffusion and intensifies the flame. Once ignition is successful, the combustion process in the pre-chamber nears its end, with the mixture near the wall beginning to combust violently. This causes significant fluctuations in both the heat release rate and pressure profile.

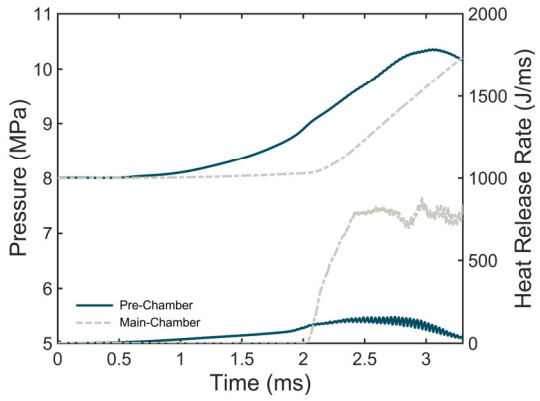

Figure 12. Pressure and heat release ate in the main-chamber and pre-chamber during the jet ignition process (hydrogen-assisted spark ignition pre-chamber)

Comparing the jet ignition processes in the two types of pre-chambers reveals some important differences. First, the time needed for successful ignition of the ammonia-air mixture in the main-chamber of the high-reactivity fuel spray ignition pre-chamber is about a quarter of that in the hydrogen-assisted spark ignition pre-chamber. The key reason for this is the hysteresis caused by flame propagation in the latter. Second, after the flame core forms, the heat release rate in the former chamber is significantly higher than in the latter. This is mainly because, in addition to the ammonia flame propagation, the jet in the high-activity fuel spray ignition pre-chamber continues to carry active components and pulls in the surrounding ammonia-air mixture. Third, the jet entrainment capacity and turbulence level in the high-activity fuel pre-chamber are higher due to the large pressure difference caused by rapid multi-point ignition. Finally, the combustion stability in the high-reactivity fuel spray ignition pre-chamber is better, with almost no pressure fluctuations.

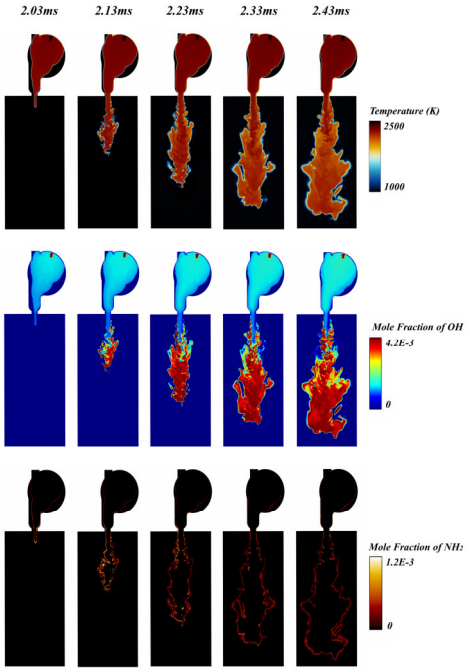

Figure 13. Thermochemical characteristics of the hydrogen-assisted spark ignition pre-chamber jet ignition process with 3 mm diameter nozzle

5 POTENTIAL FOR AMMONIA MARINE ENGINE APPLICATIONS

At the end of the paper, the potential of using high-reactivity fuel spray ignition pre-chambers for marine engine applications is examined through numerical simulations. The pre-chamber design used in the previous chapter for mechanism exploration was directly applied to our group's 130mm bore marine high-speed single-cylinder engine in this study. In this setup, the single orifice was replaced with an 8-orifice positioned obliquely to better match the shape of the combustion chamber. Computational studies were conducted at three typical loads: IMEP = 12.4 bar, 17.2 bar,

and 20.0 bar. The high-reactivity fuel spray timing was set to 10° CA BTDC.

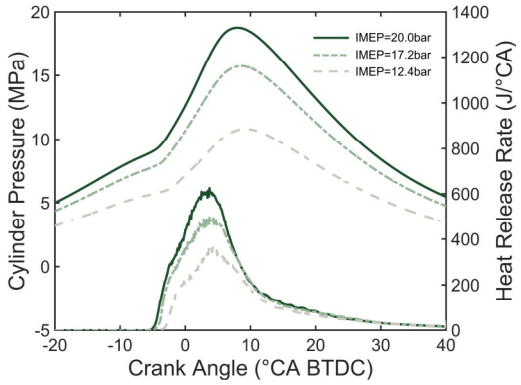

Figure 14. In-cylinder pressure and heat release rate at different loads from an ammonia engine fitted with high-reactivity fuel spray ignition pre-chamber

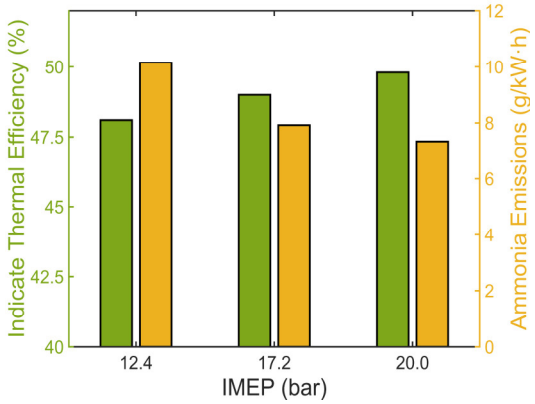

Figure 15. Indicated thermal efficiency and unburned ammonia emissions at different loads from an ammonia engine fitted with high-reactivity fuel spray ignition pre-chamber

As shown in Figure 14 and Figure 15, there is some hysteresis after the fuel is injected into the pre-chamber, which leads to the formation of multi-jet that rapidly ignites the mixture in the main-chamber. At low loads, the increasing rate of heat release rate decreases significantly after an initial rapid increase. However, this effect becomes less noticeable as the load increases. Additionally, the hysteresis between fuel injection and jet ignition is more pronounced at low loads. This suggests that the high-reactivity fuel spray ignition pre-chamber performs better at higher loads. This is also supported by thermal efficiency and emission performance analysis, which shows that the ammonia substitution rate increases from 95% to 97% as the load rises, indicating higher thermal efficiency and lower unburned ammonia emissions. When IMEP is 20.0 bar, the engine achieves an indicated thermal efficiency of 49.8% at 97% ammonia substitution, rate and unburned ammonia emissions are limited to 7.3g/kWh.

6 CONCLUSIONS

In this study, we thoroughly explored key characteristics of the high-reactivity fuel spray ignition pre-chamber through both experiments and numerical simulations. We analyzed the ignition mechanism and the potential for its application in ammonia engines, with the following main conclusions:

1. Increasing the fuel injection quantity in the pre-chamber significantly raises jet energy, reduces jet duration, and shortens the ignition lag. However, if the injection mass is increased beyond a certain point, the ultra-high equivalence ratio weakens combustion in the pre-chamber, causes significant changes in jet morphology.

2. Raising the global ammonia/air mixture equivalent ratio enhances the jet ignition process but weakens combustion in the pre-chamber.

3. The combustion process and jet properties in the pre-chamber show a staged behavior over time. The high-temperature jet formed is rich in H_2, CO, NH_3, and small-molecule hydrocarbons, but lacks sufficient oxygen.

4. The jet ignition mechanism of the high-reactivity fuel spray ignition pre-chamber involves high-temperature jets that entrain surrounding ammonia-air mixture, which then undergoes local auto-ignition, initiating the re-ignition process. The intensity of local turbulence plays a significant role. When the nozzle diameter increases from 2 mm to 3 mm, the reduction in the Karlovitz number causes the region on the Williams plot to shift from a broken reaction zone flame to a thin reaction zone, advancing the ignition time by 75%.

5. Compared to the spark ignition pre-chamber, the jet ignition in the high-reactivity fuel spray ignition pre-chamber occurs faster, the heat release rate in the main-chamber is higher, the jet entrainment capacity is stronger, and the combustion process is more stable.

6. Numerical simulation results suggest that using the high-reactivity fuel spray ignition pre-chamber could allow the high-speed marine engine to achieve an indicated thermal efficiency of 49.8% and unburned ammonia emissions of 7.3 g/kWh at high load (1500 rpm, IMEP = 20.0 bar) with 97% ammonia substitution rate.

7 ACKNOWLEDGMENTS

This work is supported by National Natural Science Foundation of China (No. U2241256, No. 52306157, No. 52394205), Key technologies research for ammonia-fueled marine engines based on the Otto cycle, Shanghai Municipal Science and Technology Major Project and Shanghai Youth Science and Technology Talents Sailing Program（23YF1419200）

8 REFERENCES

[1] Kurien, C., & Mittal, M. (2022). Review on the production and utilization of green ammonia as an alternate fuel in dual-fuel compression ignition engines. *Energy Conversion and Management*, 251, 114990.

[2] Kobayashi, H., Hayakawa, A., Somarathne, K. K. A., & Okafor, E. C. (2019). Science and technology of ammonia combustion. *Proceedings of the combustion institute*, 37(1), 109-133.

[3] Zhou, X., Li, T., Wang, N., Wang, X., Chen, R., & Li, S. (2023). Pilot diesel-ignited ammonia dual fuel low-speed marine engines: A comparative analysis of ammonia premixed and high-pressure spray combustion modes with CFD simulation. *Renewable and Sustainable Energy Reviews*, 173, 113108.

[4] Liu, L., Wu, Y., Wang, Y., Wu, J., & Fu, S. (2022). Exploration of environmentally friendly marine power technology-ammonia/diesel stratified injection. *Journal of Cleaner Production*, 380, 135014.

[5] Zhu, J., Zhou, D., Yang, W., Qian, Y., Mao, Y., & Lu, X. (2023). Investigation on the potential of using carbon-free ammonia in large two-stroke marine engines by dual-fuel combustion strategy. *Energy*, 263, 125748.

[6] Li, Z., Zhang, Z., Fan, Y., Li, J., Wu, K., Gao, Z., ... & Huang, Z. (2024). Fuel reactivity stratification assisted jet ignition for low-speed two-stroke ammonia marine engine. *International Journal of Hydrogen Energy*, 49, 570-585.

[7] Wang, X., Li, T., Chen, R., Li, S., Kuang, M., Lv, Y., ... & Lv, X. (2024). Exploring the GHG reduction potential of pilot diesel-ignited ammonia engines-Effects of diesel injection timing and ammonia energetic ratio. *Applied Energy*, 357, 122437.

[8] Mi, S., Wu, H., Pei, X., Liu, C., Zheng, L., Zhao, W., ... & Lu, X. (2023). Potential of ammonia energy fraction and diesel pilot-injection strategy on improving combustion and emission performance in an ammonia-diesel dual fuel engine. *Fuel*, 343, 127889.

[9] Trombley, G., & Toulson, E. (2023). A fuel-focused review of pre-chamber initiated combustion. *Energy Conversion and Management*, 298, 117765.

[10] Meng, X., Zhao, C., Cui, Z., Zhang, X., Zhang, M., Tian, J., ... & Bi, M. (2023). Understanding of combustion characteristics and NO generation process with pure ammonia in the pre-chamber jet-induced ignition system. *Fuel*, 331, 125743.

[11] Liu, Z., Zhou, L., & Wei, H. (2023). Experimental investigation on the performance of pure ammonia engine based on reactivity controlled turbulent jet ignition. *Fuel*, 335, 127116.

[12] Liu, Z., Zhou, L., Zhong, L., & Wei, H. (2023). Enhanced combustion of ammonia engine based on novel air-assisted pre-chamber turbulent jet ignition. *Energy Conversion and Management*, 276, 116526.

[13] Zhou, L., Zhong, L., Liu, Z., & Wei, H. (2023). Toward highly-efficient combustion of ammonia–hydrogen engine: Prechamber turbulent jet ignition. *Fuel*, 352, 129009.

[14] Wang, Z., Qi, Y., Sun, Q., Lin, Z., & Xu, X. (2024). Ammonia combustion using hydrogen jet ignition (AHJI) in internal combustion engines. *Energy*, 291, 130407.

[15] Lin, Z., Liu, S., Sun, Q., Qi, Y., & Wang, Z. (2024). Numerical investigation of multiple hydrogen injection in a jet ignition ammonia-hydrogen engine. *International Journal of Hydrogen Energy*, 77, 336-346.

[16] Pei, Y., Som, S., Pomraning, E., Senecal, P. K., Skeen, S. A., Manin, J., & Pickett, L. M. (2015). Large eddy simulation of a reacting spray flame with multiple realizations under compression ignition engine conditions. *Combustion and Flame*, 162(12), 4442-4455.

[17] Kahila, H., Wehrfritz, A., Kaario, O., & Vuorinen, V. (2019). Large-eddy simulation of dual-fuel ignition: Diesel spray injection into a lean methane-air mixture. *Combustion and Flame*, 199, 131-151.

[18] Malé, Q., Staffelbach, G., Vermorel, O., Misdariis, A., Ravet, F., & Poinsot, T. (2019). Large eddy simulation of pre-chamber ignition in an internal combustion engine. *Flow, Turbulence and Combustion*, 103, 465-483.

[19] Malé, Q., Vermorel, O., Ravet, F., & Poinsot, T. (2021). Direct numerical simulations and models for hot burnt gases jet ignition. *Combustion and Flame*, 223, 407-422.

[20] Alekseev, V. A., & Nilsson, E. J. (2024). Reduced kinetics of NH3/n-heptane: Model analysis and a new small mechanism for engine applications. *Fuel*, 367, 131464.

[21] Thorsen, L. S., Jensen, M. S., Pullich, M. S., Christensen, J. M., Hashemi, H., Glarborg, P., ... & Ju, Y. (2023). High pressure oxidation of NH3/n-heptane mixtures. *Combustion and Flame*, 254, 112785.

[22] Stagni, A., Arunthanayothin, S., Dehue, M., Herbinet, O., Battin-Leclerc, F., Bréquigny, P., ... & Faravelli, T. (2023). Low-and intermediate-temperature ammonia/hydrogen oxidation in a flow reactor: Experiments and a wide-range kinetic modeling. *Chemical Engineering Journal*, 471, 144577.

[23] Zhou, X., Li, T., Chen, R., Wei, Y., Wang, X., Wang, N., ... & Yang, W. (2024). Ammonia marine engine design for enhanced efficiency and reduced greenhouse gas emissions. *Nature Communications*, 15(1), 2110.

[24] Lin, S. P., & Reitz, R. D. (1998). Drop and spray formation from a liquid jet. *Annual review of fluid mechanics*, 30(1), 85-105.

[25] Schmidt, D. P., & Rutland, C. J. (2000). A new droplet collision algorithm. *Journal of Computational Physics*, 164(1), 62-80.

[26] Frossling, N. (1938). Uber die verdunstung fallernder tropfen. Gerlands Beitr. Geophys., 52, 170-216.

[27] O'rourke, P. J., & Amsden, A. A. (1996). A particle numerical model for wall film dynamics in port-injected engines. *SAE transactions*, 2000-2013.

[28] Han, Z., & Reitz, R. D. (1995). Turbulence modeling of internal combustion engines using RNG κ-ε models. *Combustion science and technology*, 106(4-6), 267-295.

[29] Senecal, P. K., Pomraning, E., Richards, K. J., Briggs, T. E., Choi, C. Y., McDavid, R. M., & Patterson, M. A. (2003). Multi-dimensional modeling of direct-injection diesel spray liquid length and flame lift-off length using CFD and parallel detailed chemistry. *SAE transactions*, 1331-1351.

9 CONTACT

The original manuscript writing and numerical simulation work in this paper was conducted by Zhuohang Li (Email: zhuohangli@sjtu.edu.cn), and the experimental work was carried out by Jinze Li (Email: jinze_li@sjtu.edu.cn). Both researchers contributed equally to this paper and are co-first authors.

Prof. Lei Zhu (Email: tonyzhulei@sjtu.edu.cn) is the corresponding author.